

# H19, a Long Non-coding RNA, Mediates Transcription Factors and Target Genes through Interference of MicroRNAs in Pan-Cancer

Aimin Li,<sup>1,2,9</sup> Saurav Mallik,<sup>2,9</sup> Haidan Luo,<sup>3,4</sup> Peilin Jia,<sup>2</sup> Dung-Fang Lee,<sup>2,3,5,6</sup> and Zhongming Zhao<sup>2,6,7,8</sup>

<sup>1</sup>Shaanxi Key Laboratory for Network Computing and Security Technology, School of Computer Science and Engineering, Xi'an University of Technology, Xi'an, Shaanxi 710048, China; <sup>2</sup>Center for Precision Health, School of Biomedical Informatics, The University of Texas Health Science Center at Houston, Houston, TX 77030, USA; <sup>3</sup>Department of Integrative Biology and Pharmacology, McGovern Medical School, The University of Texas Health Science Center at Houston, Houston, TX 77030, USA; <sup>4</sup>Department of Pathophysiology, Zhongshan School of Medicine, Sun Yat-sen University, Guangzhou, Guangdong 510080, China; <sup>5</sup>Center for Stem Cell and Regenerative Medicine, Brown Foundation Institute of Molecular Medicine for the Prevention of Human Diseases, The University of Texas Health Science Center at Houston, Houston, TX 77030, USA; <sup>6</sup>University of Texas MD Anderson Cancer Center UTHealth Graduate School of Biomedical Sciences, Houston, TX 77030, USA; <sup>7</sup>Human Genetics Center, School of Public Health, The University of Texas Health Science Center at Houston, Houston, TX 77030, USA; <sup>8</sup>Department of Biomedical Informatics, Vanderbilt University Medical Center, Nashville, TN 37203, USA

**Long non-coding RNAs (lncRNAs) have recently been found to be important in gene regulation. lncRNA H19 has been reported to play an oncogenic role in many human cancers. Its specific regulatory role is still elusive. In this study, we developed a novel analytic approach by integrating the synergistic regulation among lncRNAs (e.g., H19), transcription factors (TFs), target genes, and microRNAs (miRNAs) and then applied it to the pan-cancer expression datasets from The Cancer Genome Atlas (TCGA). Using linear regression models, we identified 88 H19-TF-gene co-regulatory triplets, in which 93% of the TF-gene pairs were related to cancer, indicating that our approach was effective to identify disease-related lncRNA-TF-gene co-regulation mechanisms. lncRNAs can function as miRNA sponges. Our further experiments found that H19 might regulate *SP1-TGFBR2* through *let-7b* and *miR-200b*, *ETS1-TGFBR2* through *miR-29a* and *miR-200b*, and *STAT3-KLF11* through *miR-17* in breast cancer cell lines. Our work suggests that miRNA-mediated lncRNA-TF-gene co-regulation is complicated yet important in cancer.**

## INTRODUCTION

Long non-coding RNA (lncRNA) refers to a class of transcripts that are longer than 200 nt (bp) and are not translated to protein.<sup>1</sup> lncRNA has been recently found to have many biological functions such as transcriptional regulation, epigenetic modification, and cell fate determination.<sup>2</sup> It has been involved in many diseases, including cancer.<sup>3</sup> For example, oncogenic lncRNAs may downregulate cancer cell antigen presentation and intrinsic tumor suppression,<sup>4</sup> and they can serve as potential biomarkers for cancer diagnosis and therapeutic strategy development.<sup>5,6</sup> Among thousands of lncRNA molecules discovered so far, H19 is one that is highly expressed.<sup>7-9</sup> Accumulating data have suggested that lncRNA H19 plays a critical role in tumor initiation, progression, and recurrence in various human cancers.<sup>10</sup> H19 has been reported to control cell cycle progression

through regulating RB-E2F signaling in colorectal cancer.<sup>11</sup> It plays an essential role in the exosome-mediated phenotype of endothelial liver cancer cells.<sup>12</sup> H19 competitively binds a microRNA, miR-17-5p, to regulate *YES1* gene expression in thyroid cancer.<sup>13</sup> Moreover, H19-derived miR-675 contributes to bladder cancer cell proliferation through regulating p53 activity.<sup>14</sup>

lncRNA can act as a competing endogenous RNA (ceRNA) to interact with other protein-coding RNA transcripts, both transcription factor (TF) and non-TF genes.<sup>15,16</sup> Hereafter, we refer to genes as protein-coding genes to separate them from non-coding genes. By sharing the common miRNA-binding sites with mRNAs or directing miRNA degradation, lncRNA competes with the miRNA target genes (TFs or non-TF genes) through interacting with miRNA; consequently, the expression of miRNA-targeted genes will be upregulated. This type of lncRNA-miRNA-gene competing co-regulation (triplets) has been discovered in humans and several other species.<sup>17</sup> lncRNA may also interfere with the classic TF-gene regulation by acting as a ceRNA.

Although lncRNA is important in cancer, how it plays its regulatory roles in the complex and dynamic cellular systems remains largely unknown, especially at the pan-cancer level. In this work, we developed

Received 18 January 2020; accepted 22 May 2020;  
<https://doi.org/10.1016/j.omtn.2020.05.028>.

<sup>9</sup>These authors contributed equally to this work.

**Correspondence:** Zhongming Zhao, Center for Precision Health, School of Biomedical Informatics, The University of Texas Health Science Center at Houston, Houston, TX 77030, USA.  
**E-mail:** [zhongming.zhao@uth.tmc.edu](mailto:zhongming.zhao@uth.tmc.edu)

**Correspondence:** Dung-Fang Lee, Department of Integrative Biology and Pharmacology, McGovern Medical School, The University of Texas Health Science Center at Houston, Houston, TX 77030, USA.  
**E-mail:** [dung-fang.lee@uth.tmc.edu](mailto:dung-fang.lee@uth.tmc.edu)



an analytical strategy to explore the synergistic regulation among lncRNAs, miRNAs, TFs, and genes. We applied this approach to The Cancer Genome Atlas (TCGA) pan-cancer datasets. We specifically examined H19, one of the highly expressed lncRNAs in cancer (Figure S1). Among the 24 cancer types we examined, we found that H19 was highly expressed in 21 cancer types, although not in the other three types (lower grade glioma [LGG], prostate adenocarcinoma [PRAD], and thyroid carcinoma [THCA]). As mentioned above, lncRNA might act as miRNA sponges to play roles in TF-gene regulation. Thus, we hypothesized that H19 could mediate TF-gene regulation through controlling miRNAs. After investigating the regulatory relationship among H19, miRNAs, TFs, and genes, we pinpointed three co-regulation triplets (H19-SP1-*TGFBR2*, H19-ETS1-*TGFBR2*, and H19-STAT3-*KLF11*) to validate our hypothesis in breast cancer cell lines. Our experimental results revealed that H19 might mediate (1) SP1-*TGFBR2* (TF-gene) interaction through let-7b and miR-200b, (2) ETS1-*TGFBR2* (TF-gene) interaction through miR-29a and miR-200b, and (3) STAT3-*KLF11* (TF-gene) interaction through miR-17. Such regulatory triplets can be used to predict the potential function of lncRNAs and miRNAs in cancer. Our study showed that lncRNA could interfere with miRNA-mediated TF-gene interactions. This critical regulation, if universal in various cancer types, will be important for understanding the molecular mechanisms of cancer initiation and progression, and the molecules included in the interaction can serve as biomarkers for cancer diagnosis, drug development, and therapeutic strategy development.

## RESULTS

### Classifying Samples by H19 Expression Level

lncRNA H19 is highly expressed in many cancer types and is actively involved in all stages of tumorigenesis.<sup>10</sup> To better understand the role of H19 in cancer, we analyzed the expression level of H19 in TCGA pan-cancer datasets and grouped the samples into “low,” “middle,” and “high” by H19 expression level. For instance, in breast invasive carcinoma (BRCA) samples, we reordered all of the samples by H19 expression and named the top 25% as the high group and the bottom 25% as the low group of H19 expression (Figure 1A). Taking the same criterion, we evaluated the H19 expression level in the remaining 23 cancer types and found that 25% is an appropriate percentage to set as the threshold (Table S1; Figure 2). In most of these 24 cancer types, the H19 expression profile within the middle 50% of samples showed a steady line with a mild slope. This indicated that these samples had similar and stable levels of H19 expression. However, outside the middle section, the profile lines showed significant change at the inflection points. As shown in Figure 2, samples falling into the zone from zero to the end point of rapid increases (the red vertical solid line) are considered as the H19 low group, whereas samples with the H19 level in the top section, from the start of dramatic increases (the blue vertical dashed line) to the end, are designated as the H19 high group. Interestingly, in a previous study, Li et al.<sup>18</sup> also used the 25th percentile as the threshold for dividing the top and bottom samples in their study. After having these cutoff thresholds, we further identified the H19 class labels of samples for BRCA TF expression data.

### Identification of H19-TF-Gene Triplets

We first focused on explaining the results from TCGA BRCA samples; the results of other cancer types are provided in Table S1. Based on the FPKM (fragments per kilobase of exon per million mapped reads) score, we filtered out 694 TFs and 11,867 non-TF genes from TCGA BRCA dataset. Using two databases, TRANSFAC (release 2016.4)<sup>19</sup> and TRRUST (version 2.0),<sup>20</sup> we obtained a total of 13,263 TF-target gene pairs (interactions), of which 8,181 TF-target gene pairs (interactions) were found to be expressed (FPKM score of at least 50% of samples was greater than 1) in these samples, corresponding to 625 unique TFs and 2,198 unique non-TF genes.

To evaluate the impact of H19 on TF-gene regulation, we used linear regression to obtain the expression profile of TFs and genes after excluding the effect of copy number variations (CNVs) on their expression (Figure 1B; Equation 1). Next, these new expression profiles were fed to the second linear regression model (Figure 1B; Equation 2) to assess the effect of H19 on TF or gene expression. In BRCA, 679 TF-gene regulation interactions were found to be affected by H19 (required both false discovery rate [FDR]<sub>EXPTF,ξ;GroupH19</sub> < 0.05 and  $P_{EXPTF,ξ}$  < 0.05) (Table 1). Of note, to reduce the false-positive rate (FDR), we required that these significant H19-TF-gene triplets should present in at least two TCGA cancer types. By following the analysis procedure above, we obtained a total of 88 triplets (Table S2). Figure 3 demonstrates the four most significant triplets ( $-\log_{10}(P_{EXPTF,ξ}) > 9$ ) whose TF-gene regulation was affected by the change of H19 expression. The remaining triplets are presented in Figure S2. In Figure 3, all TF-gene regulations affected by the change of H19 expression were statistically significant (FDR < 0.05). For instance, in the presence of high H19 expression, the correlation between MYBL2 and COL1A1 was significantly changed (positive correlation with  $p = 3.31 \times 10^{-3}$  to negative correlation with  $p = 2.74 \times 10^{-10}$ ).

We found that 173 of 186 (93%) TF-gene pairs had direct or indirect evidence to support their relationship to cancer (Table S3). According to this high rate, we thought that the remaining 13 TF-gene pairs might play roles in cancer as well and warrant further studies. These 13 TF-gene pairs are as follows: LUAD, CTCF-*IPO13*; KIRC, SP3-*EDF1*; PAAD, USF1-*FMRI*; STAD, EZH2-*DACT3*; TGCT, FOXO1-*HYOU1*; THCA, CTCF-*IPO13*, NFKB1-*CHUK*, NFYB-*EDF1*, RELA-*BGN*, RUNX1-*SYMPK*, SP1-*ME1*, SP1-*SIGIRR*, and SP3-*EDF1*. Interestingly, most of them (8 out of 13) were found in THCA, suggesting that this cancer type might have additional regulatory roles. These results indicate that our approach is effective in identifying TFs or genes that are related to cancer.

### H19 Regulates TF-Gene Function through the Related miRNAs

Given that one of the important lncRNA functions is modulating miRNAs, we speculated that H19 might mediate TF-gene interactions through the regulation of miRNAs. Through a comprehensive literature search (Table S4), we identified 29 miRNAs (let-7a, let-7b, let-7g, let-7i, miR-106a, miR-130b-3p, miR-138-5p, miR-139, miR-141, miR-152-3p, miR-152-5p, miR-17-5p, miR-181d-3p, miR-181d-5p,

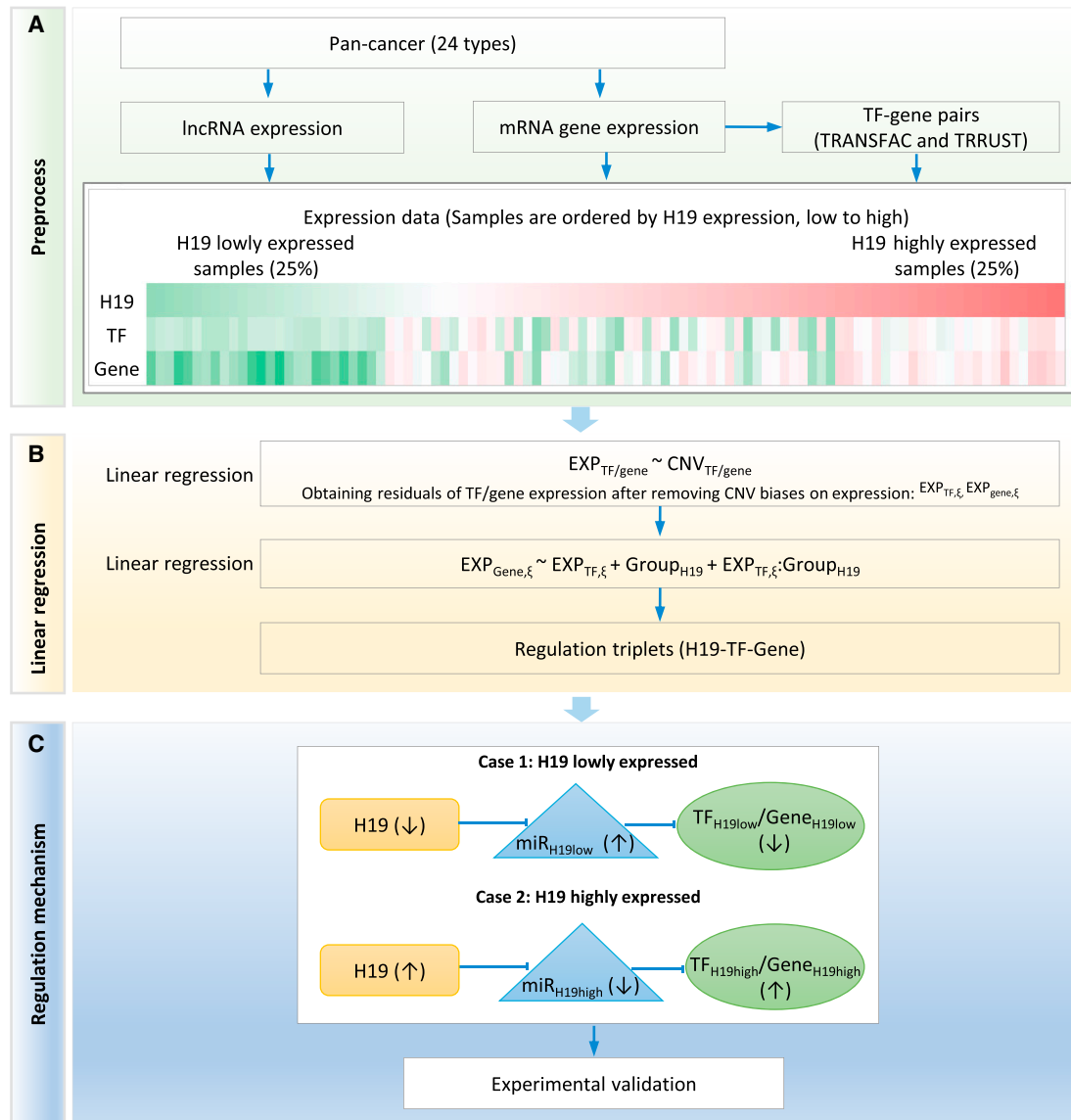


**Figure 1. Analytical Pipeline for Identification of lncRNA-TF-Gene Triplets and H19 Is Used as an Example**

(A) Analysis of lncRNA, TF and gene expression, followed by ordering the samples according to H19 expression. Expression data for lncRNAs, TFs, and genes in 24 cancer types were extracted from TCGA. TF-gene interaction pairs were retrieved from two databases, TRANSFAC and TRRUST. On each plot, samples were ordered by H19 expression from low to high. Samples that were within 25% of the lowly (highly) expressed samples were considered as a lowly (highly) expressed group. (B) Linear regression analysis of H19 expression with the TF-gene pairs, leading to H19-TF-gene triplets. The effect of copy number variation (CNV) on gene expression was filtered out. (C) Test of the hypothesis that H19 may act as a miRNA sponge in lncRNA-TF-gene triplet regulation. In the low expression H19 case, loss of H19 weakens the inhibition of miRNAs, leading to the downregulation of miRNA target TFs and/or genes; in the high expression H19 case, enhanced H19 inhibits miRNA expression, leading to upregulation of miRNA target TFs and/or genes. ↑, Upregulated; ↓, downregulated.

miR-18a, miR-194-5p, miR-196a, miR-19a, miR-19b-1, miR-200b, miR-200c, miR-20a, miR-22, miR-29a, miR-29b, miR-342-3p, miR-630, miR-874, and miR-92a-1) that were targeted by H19 (Table S4). Next, miRNA target genes of these 29 miRNAs were collected from the miRNA target prediction databases using the SpidermiR R tool.<sup>21</sup> Among these target genes, 85 overlaid with the H19-TF-gene triplets that we identified in the earlier regression analysis. We

selected eight triplets (H19-ETS1-*TGFBR2*, H19-FLI1-*TGFBR2*, H19-FOXO1-*TXNIP*, H19-KLF6-*TXNIP*, H19-NFYB-*SP3*, H19-PPARA-*KLF11*, H19-SP1-*TGFBR2*, and H19-STAT3-*KLF11*) and investigated the impact of these 29 miRNAs on them (Table S5). After having confirmed the target TF and non-TF genes of the H19-mediated miRNAs, we mainly focused on two cases (cases 1 and 2) in BRCA (Figure 1C).

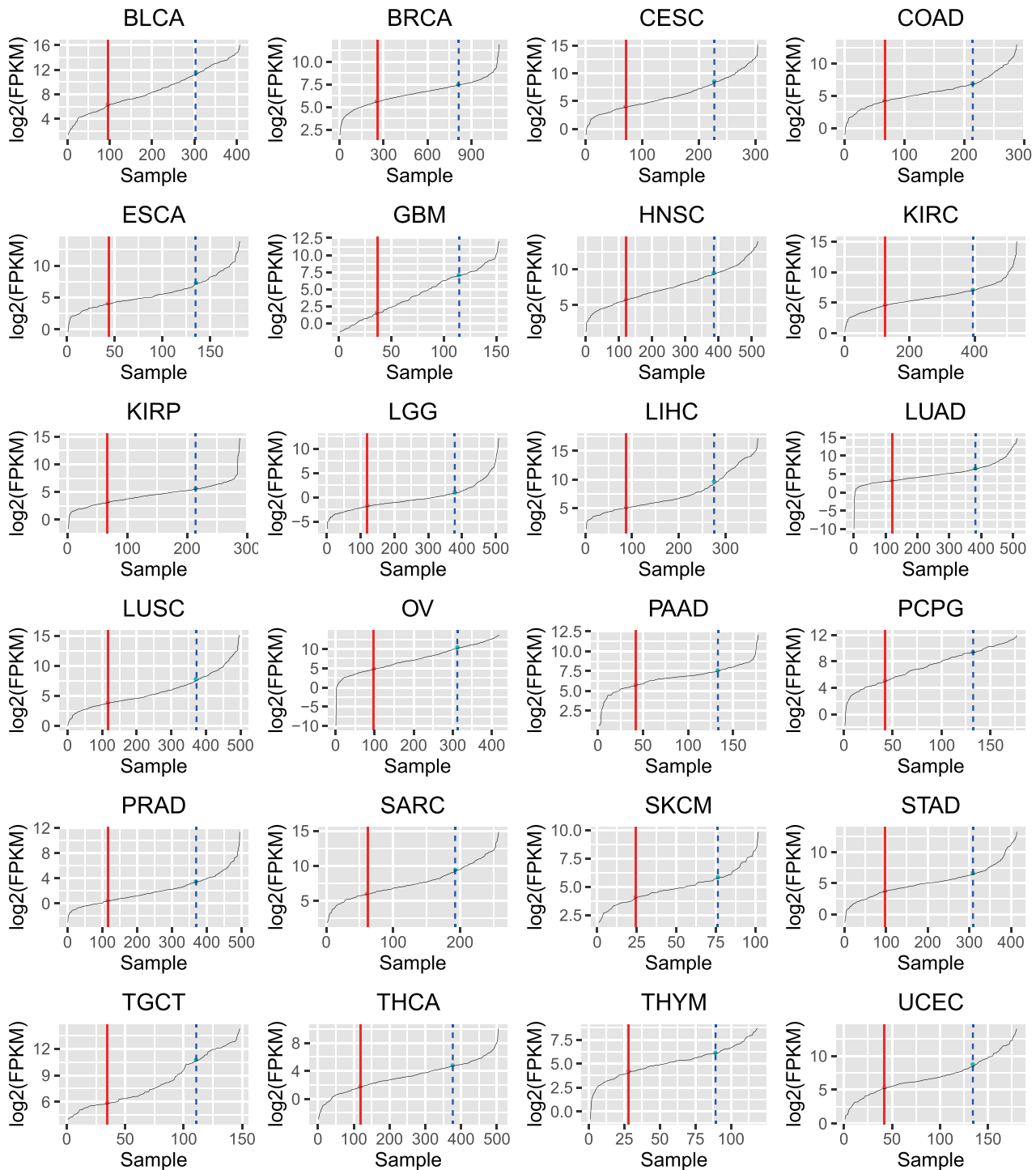


**Figure 2. All Tested Cancer Types, with Samples Classified into Low, Moderate, and High Expression Groups by H19 Level**

Twenty-four cancer types are represented. Classifications of samples are shown as low (left of the solid line), moderate (middle), and high (right of the dotted line).

**Table 1. TF-gene Regulation Interactions Significantly Affected by the Expression Alteration of H19**

Cancer Type	Number		TF-Gene Pairs	TF-Gene Pairs (FDR < 0.05) <sup>a</sup>	Triplets <sup>b</sup>
	TFs	Genes			
BLCA	607	2,103	7,723	1	0
BRCA	625	2,198	8,181	874	679
CESC	634	2,161	8,057	0	0
COAD	631	2,187	8,123	148	123
ESCA	655	2,205	8,277	3	1
GBM	636	2,156	7,755	2	0
HNSC	621	2,140	7,866	78	49
KIRC	628	2,172	7,889	246	160
KIRP	591	2,030	7,130	12	5
LGG	589	1,996	6,837	179	112
LIHC	546	1,964	6,988	2	1
LUAD	621	2,233	8,223	610	462
LUSC	653	2,281	8,444	0	0
OV	622	2,159	8,030	0	0
PAAD	651	2,369	8,758	1,165	945
PCPG	562	1,896	6,438	1	0
PRAD	624	2,170	7,889	1	0
SARC	602	2,053	7,353	24	13
SKCM	585	1,982	7,055	0	0
STAD	648	2,252	8,460	207	159
TGCT	620	2,202	8,042	574	466
THCA	587	2,020	7,284	1,095	916
THYM	602	2,055	7,270	0	0
UCEC	625	2152	8,092	0	0

<sup>a</sup>Number of TF-gene pairs with regression FDR < 0.05.  
<sup>b</sup>Number of triplets after CNV filtration.

**Case 1**

First, we chose 56 matched (common) H19 low expression group samples along with the corresponding 56 matched normal samples from TCGA BRCA miRNA/TF/non-TF gene expression database. Next, we applied the limma-voom R statistical tool<sup>22</sup> and obtained the lists of upregulated (UPR) and downregulated (DWR) miRNAs/TFs/non-TF genes from this pool. As the result (i.e., for the H19 low expression group samples), we identified five cases as UPRmiR<sub>H19low</sub> (let-7b,  $p = 1.51 \times 10^{-6}$ ; miR-29a,  $p = 6.77 \times 10^{-6}$ ; miR-200b,  $p = 2.67 \times 10^{-3}$ ; miR-17,  $p = 1.42 \times 10^{-2}$ ; and miR-29b,  $p = 4.49 \times 10^{-2}$ ), one case as DWRmiR<sub>H19low</sub> (miR-130b,  $p = 4.60 \times 10^{-4}$ ), five cases as DWRTF<sub>H19low</sub> (ETS1,  $p = 8.40 \times 10^{-4}$ ; PPARA,  $p = 8.16 \times 10^{-4}$ ; STAT3,  $p = 3.29 \times 10^{-8}$ ; NFYB,  $p = 4.58 \times 10^{-8}$ ; and SP1,  $p = 4.63 \times 10^{-3}$ ), and two cases as DWRTF<sub>H19low</sub> (SP3,  $p = 2.84 \times 10^{-14}$ ; and *TGFBR2*,  $p = 2.99 \times 10^{-3}$ ). Neither TFs nor genes were found as UPRTF<sub>H19low</sub> or UPRGene<sub>H19low</sub>, respectively (Table 2). The specific definitions of the terms such as

UPRmiR<sub>H19low</sub> and DWRmiR<sub>H19low</sub> are provided in [Materials and Methods](#).

**Case 2**

Similarly, we selected 40 matched cancer and normal samples in the H19 high expression group from TCGA BRCA miRNA/TF/non-TF gene expression database. The limma-voom tool was utilized to identify the upregulated and downregulated miRNAs/TFs/non-TF genes in this set. For this H19 high expression group samples, we identified two cases as UPRmiR<sub>H19high</sub> (miR-141,  $p = 5.86 \times 10^{-5}$ ; and miR-29b,  $p = 1.42 \times 10^{-2}$ ), one case as DWRmiR<sub>H19high</sub> (miR-200b,  $p = 4.45 \times 10^{-3}$ ), and four cases as DWRTF<sub>H19high</sub> (SP1,  $p = 2.06 \times 10^{-5}$ ; FL11,  $p = 5.65 \times 10^{-4}$ ; STAT3,  $p = 2.86 \times 10^{-3}$ ; and NFYB,  $p = 1.24 \times 10^{-2}$ ). Neither TFs nor genes were found as UPRTF<sub>H19high</sub>, UPRGene<sub>H19high</sub>, or DWRGene<sub>H19high</sub> (Table 2).

**Statistically Evaluated Interesting Gene Regulation Cascades of Triplets**

We proposed two scenarios to explain the regulation between every pair of two participating biomolecules within a triplet under different conditions, as follows: (1) H19 (↓)-UPRmiR<sub>H19low</sub> (↑)-DWRTF<sub>H19low</sub>/DWRGene<sub>H19low</sub> (↓): the downregulated expression of H19 causes the upregulation of its target miRNAs, which results in the downregulated expression of their target TFs or genes. (2) H19 (↑)-DWRmiR<sub>H19low</sub> (↓)-UPRTF<sub>H19low</sub>/UPRTF<sub>H19low</sub> (↑): the upregulated expression of H19 causes the downregulation of its target miRNAs, which in turn causes upregulated expression of their target TFs or genes. Accordingly, we found five triplets that met the regulation scenarios above: (1) H19 (↓)-let-7b (↑)-SP1 (↓)-*TGFBR2* (↓); (2) H19 (↓)-miR-29a (↑)-ETS1 (↓)-*TGFBR2* (↓); (3) H19 (↓)-miR-200b (↑)-ETS1 (↓)-*TGFBR2* (↓); (4) H19 (↓)-miR-200b (↑)-SP1 (↓)-*TGFBR2* (↓); and (5) H19 (↓)-miR-17 (↑)-STAT3 (↓)-*KLF11* (↓). If we could prove that the status changes met our prediction, it would be helpful to improve the network validation and understanding the overall effect on expression patterns of the miRNAs/TFs/genes due to different expression levels of H19.

**Experimental Validation**

In order to examine whether H19 serves as a mRNA sponge to regulate the expression of TFs and their downstream targets through antagonizing let-7b, miR-17, miR-200b, and miR-29a,<sup>13,23–28</sup> breast cancer cell lines BT-549, HCC38, MCF7, and MDA-MB-231 were used with ectopically expressing inducible H19.<sup>29</sup> Compared to the control cells, the overexpression of H19 could upregulate the distinct levels of mRNA expression of let-7b/miR-200b-regulated SP1, miR-29a/miR-200b-regulated ETS1, and miR-17-regulated STAT3 in the breast cancer cell lines (Figures 4A–4D). Consequently, the expression of the SP1/ETS1 transcriptional target *TGFBR2* and STAT3 target *KLF11* was also increased to different extents upon H19 induction. However, there was no obvious induction of *TGFBR2* detected in BT549 or MD-MB231 cells, which could be due to the low expression of SP1 and ETS in such cells or dysregulation of other transcriptional co-regulators (Figures 4A and 4C). Taken together, these lines of experimental evidence support our notion of miRNA-mediated

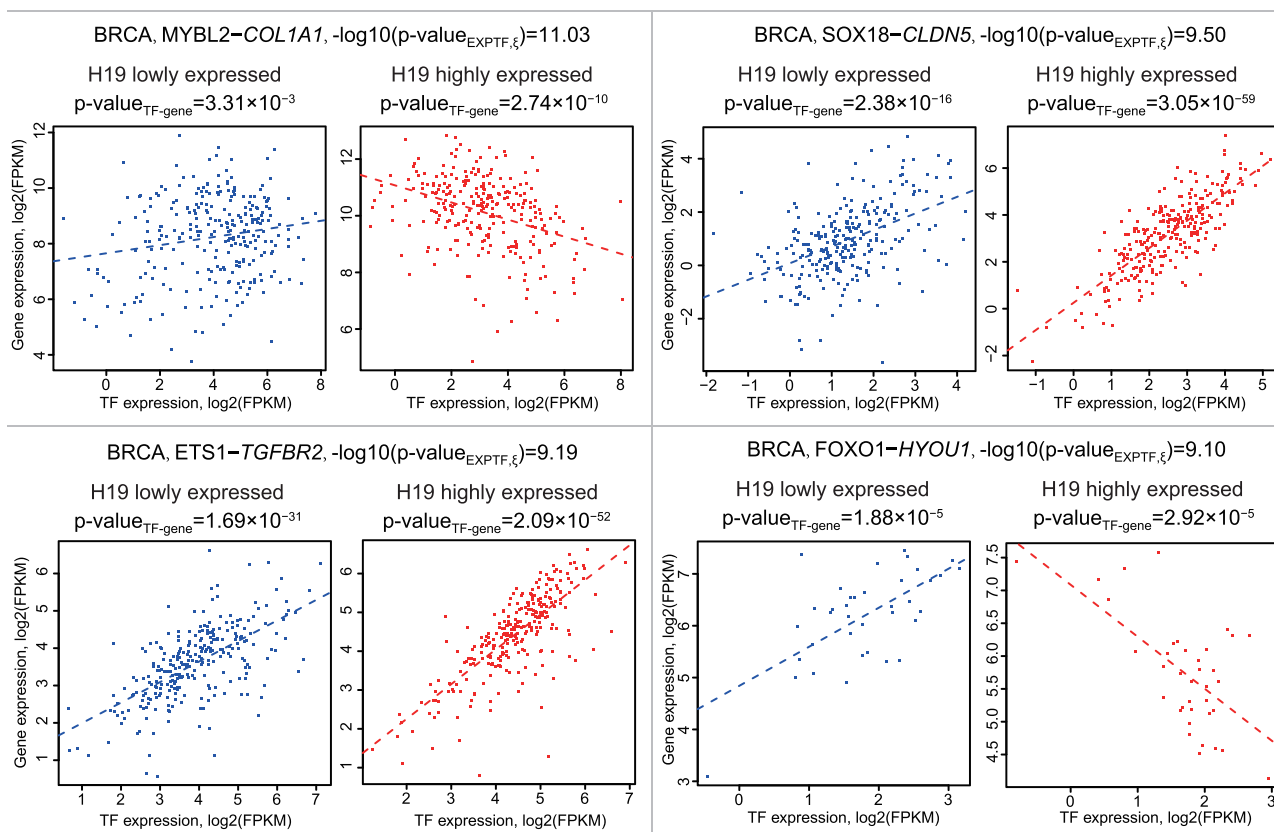


**Figure 3. TF-Gene Regulation as Affected by H19 Expression Level**

Linear regression was used to evaluate the association between TF expression and its target gene expression.

H19-TF-gene triplet regulation, indicating that H19 upregulates transcription factors and their downstream effects by sequestering miRNAs in cancer.

## DISCUSSION

Identification of cancer-associated lncRNAs and uncovering their molecular mechanisms are currently challenging but important tasks. Traditionally, studies of gene expression deregulation and alterations in genomic sequences in tumor cells have led to the identification of cancer-associated lncRNAs.<sup>5,30</sup> Subsequent *in vitro* and *in vivo* studies have directly associated some of the identified lncRNAs with specific cancer phenotypes. In this study, we identified 88 H19-TF-gene triplets based on TCGA pan-cancer data using linear regression models. Most of these TF-gene pairs (93%) had direct or indirect evidence to support their relationship to cancer (Table S3). The remaining TF-gene pairs could serve as potential candidates and warrant further investigation. Our results demonstrate that this analytical, co-regulation-based approach is promising to identify TFs or genes related to cancer. To investigate the potential regulatory mechanism, we hypothesized that H19 acts as a miRNA sponge to diminish certain miRNAs, which in turn preserves the corresponding TF-gene function. Our quantitative real-time PCR experimental results suggest that H19 mediates SP1-TGFB2 (TF-gene) regulation

through let-7b and miR-200b (miRNA), ETS1-TGFB2 regulation through miR-29a and miR-200b, and STAT3-KLF11 regulation through miR-17 in BT-549, HCC38, MCF7, and MDA-MB-231 breast cancer cell lines. Our approach can help identify lncRNAs, miRNAs, TFs, and genes that are potentially cancer associated and uncover their complex regulatory mechanisms. This approach effectively extends the previous miRNA-TF-gene co-regulation approach that has been well studied in various cancer types or other disease.<sup>31-33</sup>

TRANSFAC and TRRUST are representative databases for annotations of TF-target gene pairs. The annotations are based on stringent criteria, including both experimental evidence and statistical tests. After filtration, we obtained 13,263 TF-target gene pairs from these two databases. Although the number of TF-gene pairs is smaller than that from other databases, such as ENCODE,<sup>34</sup> we decided to use them for reducing false-positive results. For the large-scale data analysis, false-positive data would have more potential problems than false-negative data, while our goal is to find those enriched signals (e.g., regulatory networks) that have reliable evidence.

The samples studied were classified into three groups by H19 expression, that is, low, middle, and high. In such a way, we could

**Table 2. Genes, TFs, and miRNAs Were Upregulated or Downregulated.**

Group	Molecule	Log <sub>2</sub> FC	p	Regulation	
H19 lowly expressed	miRNA	let-7b	0.92885	$1.51 \times 10^{-6}$	upregulated
		miR-130b	-3.6149	$4.60 \times 10^{-4}$	downregulated
		miR-17	0.90485	$1.42 \times 10^{-2}$	upregulated
		miR-200b	2.54065	$2.67 \times 10^{-3}$	upregulated
		miR-29a	1.903	$6.78 \times 10^{-6}$	upregulated
		miR-29b-2	2.4692	$4.49 \times 10^{-2}$	upregulated
		ETS1	-1.66925	$8.41 \times 10^{-4}$	downregulated
	TF	NFYB	-2.8769	$4.58 \times 10^{-8}$	downregulated
		PPARA	-2.2694	$8.16 \times 10^{-4}$	downregulated
		SP1	-0.89175	$4.64 \times 10^{-3}$	downregulated
		SP3	-1.1854	$2.85 \times 10^{-14}$	downregulated
	gene	STAT3	-1.9026	$3.29 \times 10^{-8}$	downregulated
		<i>TGFBR2</i>	-2.41715	$3.00 \times 10^{-3}$	downregulated
H19 highly expressed	miRNA	miR-141	1.12925	$5.86 \times 10^{-5}$	upregulated
		miR-200b	-2.5865	$4.46 \times 10^{-3}$	downregulated
		miR-29b-2	1.13575	$1.42 \times 10^{-2}$	upregulated
	TF	NFYB	-1.8413	$1.25 \times 10^{-2}$	downregulated
		SP1	-0.9865	$2.07 \times 10^{-5}$	downregulated
		SP3	0.0436	$6.47 \times 10^{-8}$	upregulated
		STAT3	-1.3972	$2.86 \times 10^{-3}$	downregulated
	gene	<i>KFLI1</i>	-0.992	$5.65 \times 10^{-4}$	downregulated

FC, fold change.

observe the TF-gene status change along with the changes of H19 expression. For example, we used linear regression to describe the association between ETS1 (TF) expression and *TGFBR2* expression. The p values of linear regression were  $1.69 \times 10^{-31}$  in the H19 low expression group and  $2.09 \times 10^{-52}$  in the H19 high expression group. Additionally, this classification method significantly improved ETS1-*TGFBR2* regulation ( $p < 10^{-9}$ ). This suggests that such an integrative grouping approach is effective in investigating the relationship between variation of lncRNA expression and TF-gene regulation.

Figure 2 shows a smooth slope of the curves for the patients with intermediate levels of H19 expression. This is because all of the samples were ordered by their H19 expression, and most of these samples had H19 expression without large fluctuation. For the H19 highly or lowly expressed groups, the curves displayed sharp slopes. These sharp slopes suggested that H19 was expressed with strong variation in these two groups, which is biologically useful to investigate the effect of H19 expression changes on TF-gene regulation.

Linear regression is a widely used approach to predict the output values of a biological process under specific conditions.<sup>35,36</sup> Some studies use linear regression to predict the expression of genes.<sup>37</sup> However, to our knowledge, there are few studies that use linear regression to investigate the effect of lncRNAs on TF-gene regulation.

In this study, we used a linear regression model that was fit on non-TF gene expression changes in tumor samples as the response variable using a linear combination of the input variables, including TF expression, sample groups distinguished by H19 expression level, and interaction between TF and group (Equation 2). Within a H19-TF-gene triplet, this requires the TF to regulate the target gene, and H19 to affect TF expression and consequently regulate the target gene. Therefore, we required that such triplets should satisfy both  $FDR_{\text{EXPTF},\xi;\text{GroupH19}} < 0.05$  and  $p_{\text{EXPTF},\xi} < 0.05$ .

CNVs contribute largely to gene expression.<sup>38</sup> Structural variants, including CNVs, in cancer genomes can lead to significantly reduced or increased gene expression in cancer cells.<sup>39</sup> Therefore, we removed the effect of CNVs on gene expression and reconsidered the mediation of H19 on the TF-gene regulation relationship.

The H19-let7b-SP1-*TGFBR2* interaction we identified by our bioinformatics approach was supported by actual biological experiments (Figure 4E). The lncRNA H19 can act as a sponge to bind let-7b to mediate breast cancer cell plasticity.<sup>28</sup> The let7b-SP1 interaction was verified from chimeric reads.<sup>40</sup> DNA precipitation, electrophoretic mobility shift assays, and promoter analysis confirmed that the *TGFBR2* promoter was bound by SP1.<sup>41</sup>

We observed the expression variation of SP1 and *TGFBR2* in the presence of a high level of H19 in breast cancer cell lines. The H19-let7b-SP1-*TGFBR2* interaction can be used to elucidate such a correlation. The abnormal expression of H19 and let-7b might lead to abnormal expression of SP1 and *TGFBR2* and, consequently, lead to the development of breast cancer. The molecules included in the interaction can provide candidate diagnosis biomarkers and targets for therapy.

The synergistic regulatory relationship between lncRNAs, miRNAs, and protein-coding RNAs implemented in our approach can better infer the potential function of non-coding RNAs. The H19-let7b-SP1-*TGFBR2* interaction can be used to interpret the potential functions of lncRNAs and miRNAs (Figure 4E). In mice, an overexpression of SP1 has been reported to suppress migratory and invasive abilities of breast cancer cells.<sup>42</sup> *TGFBR2* is upregulated in basal-like breast cancer cell lines.<sup>43</sup> The minor allele homozygote (GG) of rs1078985, an intronic single nucleotide polymorphism (SNP) in *TGFBR2*, had a 24% lower risk of having breast cancer compared with major allele carriers (AG or AA).<sup>44</sup> H19 and let-7b interact with SP1 and *TGFBR2*. Therefore, H19 and let-7b might be involved in breast cancer in terms of cell migratory and invasive abilities, and they could serve as potential biomarkers. This regulation can also be verified by the following evidence in literature: (1) H19 enhances breast cancer cell proliferation through positive control by E2F1;<sup>45</sup> (2) overexpression of an ectopic H19 gene promotes the tumorigenic properties of breast cancer cells;<sup>46</sup> and (3) let-7b expression in breast cancer patients was inversely associated with tumor lymph node metastasis and patient overall survival.<sup>47</sup>

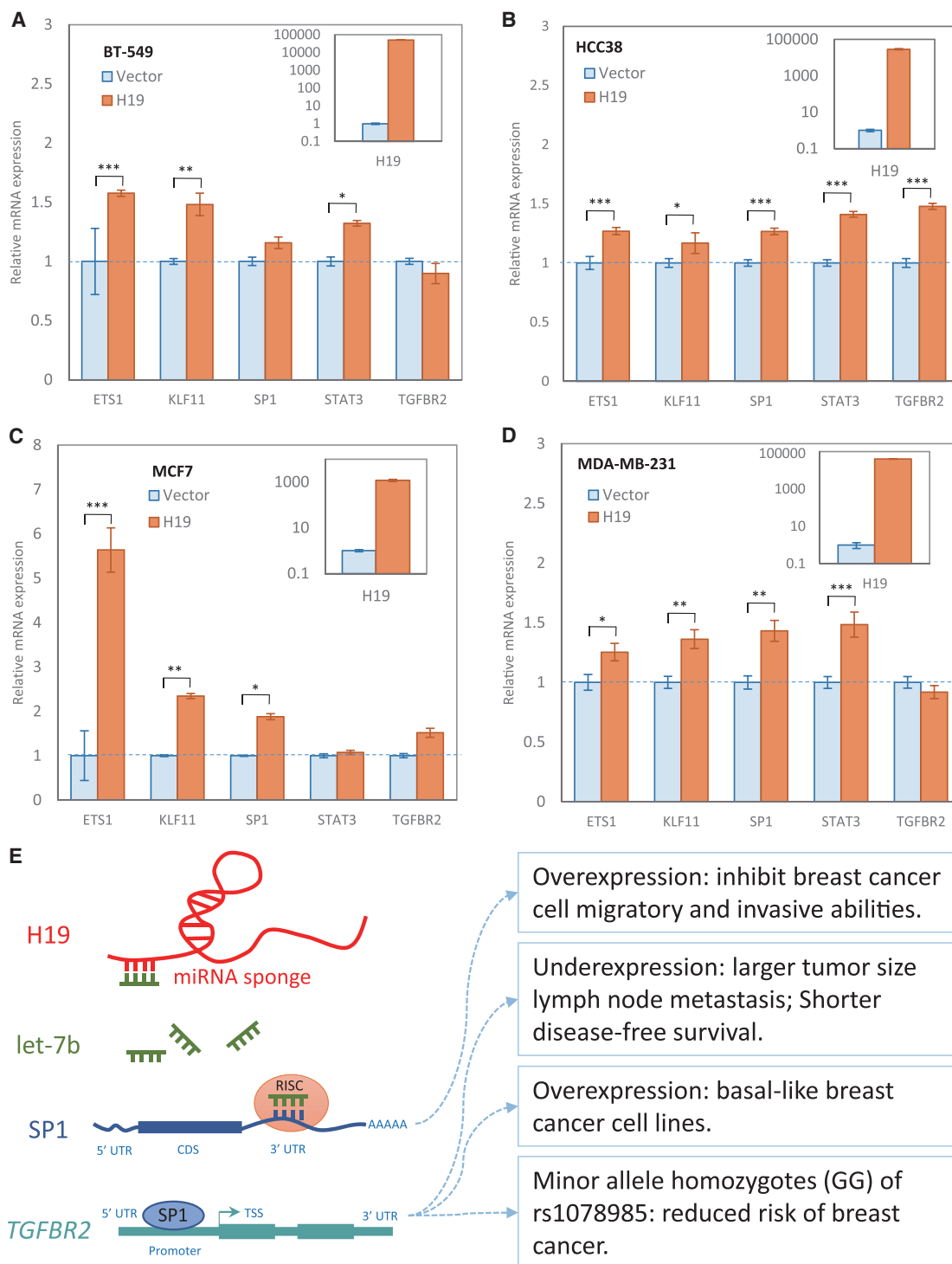


**Figure 4. H19 Functions as a miRNA Sponge to Relieve miRNA-Mediated Suppression of Transcription Factors and Their Targets**

Transcription factor targets included H19-SP1-*TGFB2*, H19-ETS1-*TGFB2*, and H19-STAT3-*KLF11*. (A–D) H19 led to an upregulated expression of let-7b/miR-17/miR-29a/miR-200b-controlled SP1, ETS1 and STAT3 (three TF genes), and their transcriptional targets *TGFB2* and *KLF11* in four breast cancer cell lines (A, BT-549; B, HCC38; C, MCF7; and D, MDA-MB-231). All samples were analyzed in triplicate and normalized to GAPDH expression. The top-right panel shows relative H19 expression. Quantitative real-time PCR data are presented as mean ± SE (standard error). \*p < 0.05, \*\*p < 0.01, \*\*\*p < 0.001. (E) The H19-let7b-SP1-*TGFB2* interaction and its

(legend continued on next page)



The study has several limitations, and there is scope for future work to be carried out. For instance, the current work only focused on one lncRNA, H19. In fact, our approach can be applied to any other lncRNAs. We focused on H19 in this study because it is one of the most promising lncRNAs and is highly expressed in most of the cancer types we examined. Moreover, this study cannot exclude false-positive results: some H19-TF-gene triplets are possibly not the real or impactful regulatory correlations, and some TFs or genes may not directly cause or be related to the specific cancer under investigation. To address this problem, we can use a lower FDR threshold to minimize a false-positive rate or validate them using various biological experiments. Finally, cancer is highly heterogeneous, and its development is dynamic in the cellular system. Our approach, like many others, cannot consider real-time or dynamic regulation in cancer and matched normal cells. However, our approach of uncovering lncRNA molecular functions contributes to identify and functionally annotate these cancer related genes, making these genes the attractive targets. These regulatory units can also better explain cancer biology. Finally, in this study, we first examined lncRNA (H19) expression in pan-cancer and then explored how it potentially regulated genes, including TF genes. Alternatively, we may analyze H19-miRNA pairs first and examine which miRNAs might be altered by H19 in the datasets. We will explore this analytical approach in the future.

## MATERIALS AND METHODS

### Data Collection

TCGA pan-cancer data consisting of 24 cancer types such as BLCA, BRCA, CESC, COAD, ESCA, GBM, HNSC, KIRC, KIRP, LGG, LIHC, LUAD, LUSC, OV, PAAD, PCPG, PRAD, SARC, SKCM, STAD, TGCT, THCA, THYM, and UCEC (full names are summarized in Table S1), whose numbers of samples were at least 90, were used for this study (Figure 1A). Tissue-specific data contained RSEM<sup>48</sup> gene FPKM data that included the lncRNA expression profile, TF expression profile, and gene (non-TF) expression profile. The data were collected through the UCSC (University of California, Santa Cruz) Xena database (<https://xenabrowser.net/>). The BRCA RSEM gene FPKM expression data contained a total of 60,499 genes and a total of 1,212 samples. For the remaining tissue-specific data, such information was provided in the UCSC Xena database (Table S1). An expression dataset of miRNAs was also collected from the UCSC Xena database. It consisted of 744 miRNAs and 10,818 samples. The curated clinical (phenotype) data that provided the list of the primary tumor samples were collected from the UCSC Xena database. In addition, the interactions between TFs and genes were collected from TRANSFAC (release 2016.4)<sup>19</sup> and TRRUST (version 2.0).<sup>20</sup> Furthermore, the interactions between miRNAs and (validated or predicted) target genes were obtained from the SpidermiR R tool<sup>21</sup> by using six target prediction databases. Among these databases, the miRTar<sup>49</sup> and miRWalk<sup>50</sup> databases provided only validated

target genes, whereas the DIANA,<sup>51</sup> miRanda,<sup>52</sup> PicTar,<sup>53</sup> and TargetScan<sup>54</sup> databases supplied predicted target genes. H19-targeted miRNAs were identified from the published literature. The detailed descriptions regarding the association of H19 and its targeted miRNAs are demonstrated in Table S4.

### Data Preprocessing

First, the biomolecules (lncRNAs, TFs, and genes) whose FPKM score of at least 50% of samples was greater than 1 were selected, whereas the remaining biomolecules were excluded from further analyses (Figure 1A). After this step, we partitioned the whole gene expression data into several subparts according to the category of the genes such as filtered TF expression data, filtered non-TF gene expression data, and filtered lncRNA (H19) expression data. The interactions between TFs and target genes were determined from two well-known databases, TRANSFAC (release 2016.4)<sup>19</sup> and TRRUST (version 2.0).<sup>20</sup> We first obtained 800 TFs and 3,470 genes from the TRANSFAC and TRRUST databases and then applied these TFs and genes to filter results from these databases and obtained 13,263 TF-target gene pairs. Using the resultant interactions, we further filtered the TF expression data in a way such that the participating (interacting) TFs belonging to the TF-gene interactions (obtained by TRANSFAC and TRRUST), which were listed in the TF expression data, were only considered in the resultant filtered TF expression data. Similarly, we again filtered the non-TF gene expression data in a way such that the target genes belonging to the TF-gene interactions that were mentioned in the non-TF gene expression data were only selected in the resultant filtered non-TF gene expression data. Next, to determine the type of expression of existing samples, we ordered the expression data of H19 underlying all of these samples based on the expression values from low to high. Here, a certain percentage of the lowly expressed samples was considered as the first group (lowly expressed group), whereas the same percentage of the highly expressed samples was treated as the second group (highly expressed group). The remaining samples were used as the third group (“middle” group). According to the resultant class labels of H19 samples, the samples of the other molecules such as gene and TF had been classified.

### Linear Regression and Copy Number Variation Factor

CNVs contribute largely to gene expression.<sup>38</sup> We removed the effect of CNVs on gene expression and then reconsidered the mediation of H19 on the TF-gene regulation relationship (Figure 1B). First, we obtained the residuals of expression of the TF and genes through the linear regression (“Stats” R tool)<sup>55</sup> using Equation 1, and then used the residuals of expression of the TF and genes to evaluate the mediation of H19 on the TF-gene regulation relationship through Equation 2 as follows:

$$EXP_{TF/Non-TF\ Gene} \sim CNV_{TF/Non-TF\ Gene}, \quad (1)$$

involvement with breast cancer. H19 acts as a miRNA sponge for let-7b that targets TF gene *SP1*. Let-7b inhibits the expression of *SP1*, whose overexpression inhibits breast cancer cell migratory and invasive abilities. *SP1* regulates *TGFBR2*, whose abnormal expression or mutation is related to breast cancer. CDS, coding DNA sequence; RISC, RNA-induced silencing complex; TSS, transcription start site; UTR, untranslated region.

where  $EXP_{TF/Gene}$  symbolizes the expression data of TF or gene, and  $CNV_{TF/Gene}$  denotes the CNV data of the TF or gene; and

$$EXP_{Non-TF\ Gene,\xi} \sim EXP_{TF,\xi} + Group_{H19} + EXP_{TF,\xi} : Group_{H19}, \quad (2)$$

where  $EXP_{Gene,\xi}$  refers to the expression data of the gene after removing the effect of CNVs,  $EXP_{TF,\xi}$  denotes the expression data of TF after removing the effect of CNVs, and  $Group_{H19}$  symbolizes the class labels of samples (low, middle, and high), whereas  $EXP_{TF,\xi}:Group_{H19}$  refers to the interaction effect between the TF and the group. Finally, we determined the triplets using the criteria (1) the adjusted p value should be less than 0.05 ( $FDR_{EXP_{TF,\xi}:Group_{H19}} < 0.05$ ), and (2) the p value corresponding to coefficient of  $EXP_{TF,\xi}$  should be less than 0.05 ( $p_{EXP_{TF,\xi}} < 0.05$ ).

### Regulatory Mechanism

After obtaining the triplets (H19-TF-gene) through linear regression, we conducted an extensive literature search to determine the interactions between H19 and miRNAs. We identified target miRNAs that interacted with H19. Next, the target genes (including TFs as well as non-TF genes) of the employing miRNAs had been identified using the SpidermiR R tool.<sup>21</sup> After finding the target genes of the H19-mediated miRNAs, we had mainly focused on two cases (Figure 1C), that is, cases 1 and 2.

#### Case 1

First we chose the matched (common) H19 lowly expressed group samples along with the matched normal samples from TCGA BRCA miRNA/TF/non-TF gene expression data. Then, we applied the limma-voom R statistical tool<sup>22</sup> to determine which miRNAs/TFs/non-TF genes were upregulated (denoted as  $UPRmiR_{H19low}$ ,  $UPR_{TFH19low}$ , and  $UPRGene_{H19low}$ , respectively), downregulated (denoted as  $DWRmiR_{H19low}$ ,  $DWR_{TFH19low}$ , and  $DWRGene_{H19low}$ , respectively), or not differentially expressed.

#### Case 2

Similarly, we selected the matched (common) H19 highly expressed group samples along with the matched normal samples from TCGA BRCA miRNA or gene expression data. Then, we used the limma-voom R statistical tool<sup>22</sup> to determine which miRNAs or genes were upregulated ( $UPRmiR_{H19high}$ ,  $UPR_{TFH19high}$ , and  $UPRGene_{H19high}$ , respectively), downregulated ( $DWRmiR_{H19high}$ ,  $DWR_{TFH19high}$ , and  $DWRGene_{H19high}$ , respectively), or not differentially expressed.

### Cell Lines

All cell lines were obtained from the American Type Culture Collection (Manassas, VA, USA), independently validated by STR DNA fingerprinting at the University of Texas MD Anderson Cancer Center (Houston, TX, USA) and determined to be negative for mycoplasma contamination. HEK293T (RRID:CVCL\_0063) cells and human breast cancer cell lines BT-549 (RRID:CVCL\_1092), HCC38 (RRID:CVCL\_1267), MCF7 (RRID:CVCL\_0031), and MDA-MB-231 (RRID:CVCL\_0062) were cultured in Dulbecco's modified Ea-

gle's medium (DMEM) with 10% fetal bovine serum (FBS) supplemented with 100 IU/mL penicillin and 100  $\mu$ g/mL streptomycin. Cells were maintained at 37°C in a humidified 5% CO<sub>2</sub> incubator.

### Generation of H19 Lentivirus and Infection

$2 \times 10^6$  HEK293T cells were seeded in 10-cm tissue culture plates and maintained in DMEM complete medium for 20 h. Media were discarded and replaced with 3 mL of Opti-MEM. 6  $\mu$ g of pCMV-dR8.2-dvpr, 2  $\mu$ g of pCMV-VSV-dvpr, 8  $\mu$ g of TetO-FUW H19<sup>29</sup> or rtTA, and 32  $\mu$ g of polyethylenimine (PEI) were added into 400  $\mu$ L of Opti-MEM. The transfection mixture was incubated at room temperature for 15 min and then added into HEK293T cells. After a 3-h incubation, 3 mL of DMEM complete medium was added. After overnight incubation, the medium was replaced with 6 mL of DMEM complete medium. The viruses were collected at 48–72 h after transfection and concentrated by Amicon Ultra-15 (Millipore). For viral infection, BT-549, HCC38, MCF7, and MDA-MB-231 cells were seeded, respectively, in six-well plates and infected with either control or H19 lentivirus. One  $\mu$ g/mL doxycycline was used to turn on the expression of H19. After 48–72 h of induction, cells were collected to examine H19, *ETS1*, *KLF11*, *SP1*, *STAT3*, and *TGFBR2* gene expression for quantitative real-time PCR.

### Quantitative Real-Time PCR

Total RNA was extracted using TRIzol reagent (Thermo Fisher Scientific, CA, USA) following the manufacturer's instructions. The RNA samples were qualified using a NanoDrop spectrophotometer (Thermo Fisher Scientific, CA, USA). 1  $\mu$ g of mRNA was used for reverse transcription using the iScript cDNA synthesis kit (Bio-Rad, CA, USA). A 20- $\mu$ L quantitative real-time PCR reaction solution was composed of 1  $\mu$ L of cDNA, 1  $\mu$ L each of 10  $\mu$ M forward and reverse qPCR primers, 10  $\mu$ L of SYBR Green PCR master mix (Bio-Rad, CA, USA), and 7  $\mu$ L of RT-PCR-grade water. qPCR reactions were performed on a CFX96 machine (Bio-Rad). All reactions were run in triplicate. The relative *ETS1*, *KLF11*, *SP1*, *STAT3*, and *TGFBR2* mRNA expression levels were normalized to their corresponding GAPDH mRNA expression. Primers used for quantitative real-time PCR detection are listed in Table S6.

### Statistical Analysis

The limma-voom R statistical tool<sup>22</sup> using an empirical Bayes statistical test was applied to identify the differentially expressed miRNAs, TFs, and non-TFs in the (common) H19 lowly or highly expressed group samples versus the matched normal samples using TCGA breast cancer gene miRNA and mRNA expression datasets. For quantitative real-time PCR, all grouped data are presented as mean  $\pm$  SE (standard error). A Student's t test was used to assess statistical significance between the two groups.

### SUPPLEMENTAL INFORMATION

Supplemental Information can be found online at <https://doi.org/10.1016/j.omtn.2020.05.028>.

## AUTHOR CONTRIBUTIONS

Z.Z. and P.J. conceived the study. A.L. and S.M. collected the data and conducted the bioinformatics analysis. H.L. and D.-F.L. conducted laboratory experiments. A.L., S.M., H.L., D.-F.L., and Z.Z. verified the results and wrote the manuscript. All authors revised and approved the final manuscript.

## CONFLICTS OF INTEREST

The authors declare no competing interests.

## ACKNOWLEDGMENTS

We thank the laboratory members of Bioinformatics and Systems Medicine Laboratory (SBML) for useful discussion, and Dr. Guangchun Han for initial analysis of lncRNA in TCGA datasets. A.L. was partially supported by the Natural Science Basic Research Plan in Shaanxi Province (2017JM6024), the Natural Science Foundation of Shaanxi Provincial Department of Education (17JK0572), and by the Teaching Research Foundation of Xi'an University of Technology (XJY1866). D.-F.L. is a CPRIT Scholar in Cancer Research and was supported by Cancer Prevention & Research Institute of Texas (CPRIT) grant RR160019. We thank the technical support from CPRIT cores (RP180734 and RP170668). The funders had no role in the study design, data collection and analysis, decision to publish, or preparation of the manuscript.

## REFERENCES

- Iyer, M.K., Niknafs, Y.S., Malik, R., Singhal, U., Sahu, A., Hosono, Y., Barrette, T.R., Prensner, J.R., Evans, J.R., Zhao, S., et al. (2015). The landscape of long noncoding RNAs in the human transcriptome. *Nat. Genet.* *47*, 199–208.
- Li, M., and Izpisua Belmonte, J.C. (2015). Roles for noncoding RNAs in cell-fate determination and regeneration. *Nat. Struct. Mol. Biol.* *22*, 2–4.
- Mitra, R., Chen, X., Greenawalt, E.J., Maulik, U., Jiang, W., Zhao, Z., and Eischen, C.M. (2017). Decoding critical long non-coding RNA in ovarian cancer epithelial-to-mesenchymal transition. *Nat. Commun.* *8*, 1604.
- Hu, Q., Ye, Y., Chan, L.-C., Li, Y., Liang, K., Lin, A., Egranov, S.D., Zhang, Y., Xia, W., Gong, J., et al. (2019). Oncogenic lncRNA downregulates cancer cell antigen presentation and intrinsic tumor suppression. *Nat. Immunol.* *20*, 835–851.
- Liu, S., Mitra, R., Zhao, M.-M., Fan, W., Eischen, C.M., Yin, F., and Zhao, Z. (2016). The potential roles of long noncoding RNAs (lncRNA) in glioblastoma development. *Mol. Cancer Ther.* *15*, 2977–2986.
- Cui, W., Qian, Y., Zhou, X., Lin, Y., Jiang, J., Chen, J., Zhao, Z., and Shen, B. (2015). Discovery and characterization of long intergenic non-coding RNAs (lincRNA) module biomarkers in prostate cancer: an integrative analysis of RNA-seq data. *BMC Genomics* *16* (Suppl 7), S3.
- Matouk, I.J., Raveh, E., Abu-lail, R., Mezan, S., Gilon, M., Gershtain, E., Birman, T., Gallula, J., Schneider, T., Barkali, M., et al. (2014). Oncofetal H19 RNA promotes tumor metastasis. *Biochim. Biophys. Acta* *1843*, 1414–1426.
- Matouk, I.O.P., Ayesh, S., Sidi, A., Czerniak, A., Groot, N.D., and Hochberg, A. (2005). The oncofetal H19 RNA in human cancer, from the bench to the patient. *Cancer Ther.* *3*, 249–266.
- Matouk, I.J., DeGroot, N., Mezan, S., Ayesh, S., Abu-lail, R., Hochberg, A., and Galun, E. (2007). The H19 non-coding RNA is essential for human tumor growth. *PLoS ONE* *2*, e845.
- Raveh, E., Matouk, I.J., Gilon, M., and Hochberg, A. (2015). The H19 long non-coding RNA in cancer initiation, progression and metastasis—a proposed unifying theory. *Mol. Cancer* *14*, 184.
- Ling, H., Ohtsuka, M., Ivan, C., Pichler, M., Chen, M., Slaby, O., Goel, A., Radovich, M., and Calin, G. (2017). Oncogenic function and molecular mechanism of H19 non-coding RNA in colorectal cancer. *Cancer Res.* *77* (Suppl), 2548. <https://doi.org/10.1158/1538-7445.AM2017-2548>.
- Conigliaro, A., Costa, V., Lo Dico, A., Saieva, L., Buccheri, S., Dieli, F., Manno, M., Raccosta, S., Mancone, C., Tripodi, M., et al. (2015). CD90<sup>+</sup> liver cancer cells modulate endothelial cell phenotype through the release of exosomes containing H19 lncRNA. *Mol. Cancer* *14*, 155.
- Liu, L., Yang, J., Zhu, X., Li, D., Lv, Z., and Zhang, X. (2016). Long noncoding RNA H19 competitively binds miR-17-5p to regulate YES1 expression in thyroid cancer. *FEBS J.* *283*, 2326–2339.
- Liu, C., Chen, Z., Fang, J., Xu, A., Zhang, W., and Wang, Z. (2016). H19-derived miR-675 contributes to bladder cancer cell proliferation by regulating p53 activation. *Tumour Biol.* *37*, 263–270.
- Wang, P., Ning, S., Zhang, Y., Li, R., Ye, J., Zhao, Z., Zhi, H., Wang, T., Guo, Z., and Li, X. (2015). Identification of lncRNA-associated competing triplets reveals global patterns and prognostic markers for cancer. *Nucleic Acids Res.* *43*, 3478–3489.
- Tay, Y., Rinn, J., and Pandolfi, P.P. (2014). The multilayered complexity of ceRNA crosstalk and competition. *Nature* *505*, 344–352.
- Salmena, L., Poliseno, L., Tay, Y., Kats, L., and Pandolfi, P.P. (2011). A ceRNA hypothesis: the Rosetta Stone of a hidden RNA language? *Cell* *146*, 353–358.
- Li, Y., Li, L., Wang, Z., Pan, T., Sahni, N., Jin, X., Wang, G., Li, J., Zheng, X., Zhang, Y., et al. (2018). LncMAP: pan-cancer atlas of long noncoding RNA-mediated transcriptional network perturbations. *Nucleic Acids Res.* *46*, 1113–1123.
- Matys, V., Kel-Margoulis, O.V., Fricke, E., Liebich, I., Land, S., Barre-Dirrie, A., Reuter, L., Chekmenev, D., Krull, M., Hornischer, K., et al. (2006). TRANSFAC and its module TRANSCOMP: transcriptional gene regulation in eukaryotes. *Nucleic Acids Res.* *34*, D108–D110.
- Han, H., Cho, J.-W., Lee, S., Yun, A., Kim, H., Bae, D., Yang, S., Kim, C.Y., Lee, M., Kim, E., et al. (2018). TRRUST v2: an expanded reference database of human and mouse transcriptional regulatory interactions. *Nucleic Acids Res.* *46* (D1), D380–D386.
- Cava, C., Colaprico, A., Bertoli, G., Graudenzi, A., Silva, T.C., Olsen, C., Noushmehr, H., Bontempi, G., Mauri, G., and Castiglioni, I. (2017). SpidermiR: an R/bioconductor package for integrative analysis with miRNA data. *Int. J. Mol. Sci.* *18*, E274.
- Law, C.W., Chen, Y., Shi, W., and Smyth, G.K. (2014). voom: precision weights unlock linear model analysis tools for RNA-seq read counts. *Genome Biol.* *15*, R29.
- Kallen, A.N., Zhou, X.-B., Xu, J., Qiao, C., Ma, J., Yan, L., Lu, L., Liu, C., Yi, J.S., Zhang, H., et al. (2013). The imprinted H19 lncRNA antagonizes let-7 microRNAs. *Mol. Cell* *52*, 101–112.
- Huang, Z., Lei, W., Hu, H.B., Zhang, H., and Zhu, Y. (2018). H19 promotes non-small-cell lung cancer (NSCLC) development through STAT3 signaling via sponging miR-17. *J. Cell. Physiol.* *233*, 6768–6776.
- Jia, P., Cai, H., Liu, X., Chen, J., Ma, J., Wang, P., Liu, Y., Zheng, J., and Xue, Y. (2016). Long non-coding RNA H19 regulates glioma angiogenesis and the biological behavior of glioma-associated endothelial cells by inhibiting microRNA-29a. *Cancer Lett.* *381*, 359–369.
- He, H., Wang, N., Yi, X., Tang, C., and Wang, D. (2017). Long non-coding RNA H19 regulates E2F1 expression by competitively sponging endogenous miR-29a-3p in clear cell renal cell carcinoma. *Cell Biosci.* *7*, 65.
- Zhou, J., Zhou, Y., and Wang, C.X. (2018). lncRNA-MIAT regulates fibrosis in hypertrophic cardiomyopathy (HCM) by mediating the expression of miR-29a-3p. *J. Cell. Biochem.* *120*, 7265–7275.
- Zhou, W., Ye, X.-L., Xu, J., Cao, M.-G., Fang, Z.-Y., Li, L.-Y., Guan, G.-H., Liu, Q., Qian, Y.-H., and Xie, D. (2017). The lncRNA H19 mediates breast cancer cell plasticity during EMT and MET plasticity by differentially sponging miR-200b/c and let-7b. *Sci. Signal* *10*, eaak9557.
- Lee, D.-F., Su, J., Kim, H.S., Chang, B., Papatsenko, D., Zhao, R., Yuan, Y., Gingold, J., Xia, W., Darr, H., et al. (2015). Modeling familial cancer with induced pluripotent stem cells. *Cell* *161*, 240–254.
- Huarte, M. (2015). The emerging role of lncRNAs in cancer. *Nat. Med.* *21*, 1253–1261.

31. Sun, J., Gong, X., Purow, B., and Zhao, Z. (2012). Uncovering microRNA and transcription factor mediated regulatory networks in glioblastoma. *PLoS Comput. Biol.* *8*, e1002488.
32. Li, A., Jia, P., Mallik, S., Fei, R., Yoshioka, H., Suzuki, A., Iwata, J., and Zhao, Z. (2019). Critical microRNAs and regulatory motifs in cleft palate identified by a conserved miRNA-TF-gene network approach in humans and mice. *Brief. Bioinform.* bbz082.
33. Mitra, R., Edmonds, M.D., Sun, J., Zhao, M., Yu, H., Eischen, C.M., and Zhao, Z. (2014). Reproducible combinatorial regulatory networks elucidate novel oncogenic microRNAs in non-small cell lung cancer. *RNA* *20*, 1356–1368.
34. ENCODE Project Consortium. (2012). An integrated encyclopedia of DNA elements in the human genome. *Nature* *489*, 57–74.
35. Zhu, Q.H., Stephen, S., Taylor, J., Helliwell, C.A., and Wang, M.B. (2014). Long non-coding RNAs responsive to *Fusarium oxysporum* infection in *Arabidopsis thaliana*. *New Phytol.* *201*, 574–584.
36. GTEx Consortium (2015). Human genomics. The Genotype-Tissue Expression (GTEx) pilot analysis: multitissue gene regulation in humans. *Science* *348*, 648–660.
37. Chiang, C., Scott, A.J., Davis, J.R., Tsang, E.K., Li, X., Kim, Y., Hadzic, T., Damani, F.N., Ganel, L., Montgomery, S.B., et al.; GTEx Consortium (2017). The impact of structural variation on human gene expression. *Nat. Genet.* *49*, 692–699.
38. Stranger, B.E., Forrest, M.S., Dunning, M., Ingle, C.E., Beazley, C., Thorne, N., Redon, R., Bird, C.P., de Grassi, A., Lee, C., et al. (2007). Relative impact of nucleotide and copy number variation on gene expression phenotypes. *Science* *315*, 848–853.
39. Jia, P., and Zhao, Z. (2017). Impacts of somatic mutations on gene expression: an association perspective. *Brief. Bioinform.* *18*, 413–425.
40. Helwak, A., Kudla, G., Dudnakova, T., and Tollervey, D. (2013). Mapping the human miRNA interactome by CLASH reveals frequent noncanonical binding. *Cell* *153*, 654–665.
41. Song, K., Wang, H., Krebs, T.L., Kim, S.-J., and Danielpour, D. (2008). Androgenic control of transforming growth factor- $\beta$  signaling in prostate epithelial cells through transcriptional suppression of transforming growth factor- $\beta$  receptor II. *Cancer Res.* *68*, 8173–8182.
42. Li, L., Gao, P., Li, Y., Shen, Y., Xie, J., Sun, D., Xue, A., Zhao, Z., Xu, Z., Zhang, M., et al. (2014). JMJD2A-dependent silencing of Sp1 in advanced breast cancer promotes metastasis by downregulation of DIRAS3. *Breast Cancer Res. Treat.* *147*, 487–500.
43. Breunig, C., Erdem, N., Bott, A., Greiwe, J.F., Reinz, E., Bernhardt, S., Giacomelli, C., Wachter, A., Kanthelhardt, E.J., Beifßbarth, T., et al. (2018). TGF $\beta$ 1 regulates HGF-induced cell migration and hepatocyte growth factor receptor MET expression via C-ets-1 and miR-128-3p in basal-like breast cancer. *Mol. Oncol.* *12*, 1447–1463.
44. Ma, X., Beeghly-Fadiel, A., Lu, W., Shi, J., Xiang, Y.-B., Cai, Q., Shen, H., Shen, C.Y., Ren, Z., Matsuo, K., et al. (2012). Pathway analyses identify *TGFBR2* as potential breast cancer susceptibility gene: results from a consortium study among Asians. *Cancer Epidemiol. Biomarkers Prev.* *21*, 1176–1184.
45. Berteaux, N., Lottin, S., Monté, D., Pinte, S., Quatannens, B., Coll, J., Hondermarck, H., Cury, J.J., Dugimont, T., and Adriaenssens, E. (2005). *H19* mRNA-like noncoding RNA promotes breast cancer cell proliferation through positive control by E2F1. *J. Biol. Chem.* *280*, 29625–29636.
46. Lottin, S., Adriaenssens, E., Dupressoir, T., Berteaux, N., Montpellier, C., Coll, J., Dugimont, T., and Cury, J.J. (2002). Overexpression of an ectopic *H19* gene enhances the tumorigenic properties of breast cancer cells. *Carcinogenesis* *23*, 1885–1895.
47. Ma, L., Li, G.Z., Wu, Z.S., and Meng, G. (2014). Prognostic significance of let-7b expression in breast cancer and correlation to its target gene of BSG expression. *Med. Oncol.* *31*, 773.
48. Li, B., and Dewey, C.N. (2011). RSEM: accurate transcript quantification from RNA-seq data with or without a reference genome. *BMC Bioinformatics* *12*, 323.
49. Hsu, J.B.-K., Chiu, C.-M., Hsu, S.-D., Huang, W.-Y., Chien, C.-H., Lee, T.-Y., and Huang, H.D. (2011). miRTar: an integrated system for identifying miRNA-target interactions in human. *BMC Bioinformatics* *12*, 300.
50. Dweep, H., Sticht, C., Pandey, P., and Gretz, N. (2011). miRWalk—database: prediction of possible miRNA binding sites by “walking” the genes of three genomes. *J. Biomed. Inform.* *44*, 839–847.
51. Maragkakis, M., Vergoulis, T., Alexiou, P., Reczko, M., Plomaritou, K., Gousis, M., Kourtis, K., Koziris, N., Dalamagas, T., and Hatzigeorgiou, A.G. (2011). DIANA-microT Web server upgrade supports Fly and Worm miRNA target prediction and bibliographic miRNA to disease association. *Nucleic Acids Res.* *39*, W145–8.
52. Enright, A.J., John, B., Gaul, U., Tuschl, T., Sander, C., and Marks, D.S. (2003). MicroRNA targets in *Drosophila*. *Genome Biol.* *5*, R1.
53. Krek, A., Grün, D., Poy, M.N., Wolf, R., Rosenberg, L., Epstein, E.J., MacMenamin, P., da Piedade, I., Gunsalus, K.C., Stoffel, M., and Rajewsky, N. (2005). Combinatorial microRNA target predictions. *Nat. Genet.* *37*, 495–500.
54. Bartel, D.P. (2009). MicroRNAs: target recognition and regulatory functions. *Cell* *136*, 215–233.
55. Pinheiro, J., Bates, D., DebRoy, S., and Sarkar, D. (2007). Linear and nonlinear mixed effects models. R package version 3, 1–89, <https://cran.r-project.org/web/packages/nlme/index.html>.